FACTA UNIVERSITATIS
Series: **Mechanical Engineering** Vol. 11, N^{o} 2, 2013, pp. 141 - 151

POTENTIAL STRAIN ENERGY SURFACES AT THE CRACK TIP VICINITY

UDC 531-3:621

Dragan B. Jovanović

Faculty of Mechanical Engineering, University of Niš, Serbia

Abstract *Results of the potential strain energy surfaces reconstruction in the region of crack as well as the basic procedures of the reconstruction method are presented. Relevant limitations and specifications of the method are pointed out while evaluating the best fitting curves and the best fitting three-dimensional surfaces of stress components and potential strain energy. Examples of cracks named in the paper as PR-Z-16 and PR-P-22, with exactly the same geometry of crack and plate are analyzed. The same finite element lattice for calculation in both cases is selected. The first example of a plate is loaded with σ in y - direction on the outer border of the plate, perpendicularly on the plane of crack, while in the example PR-P-22 the plate is loaded with σ continually and perpendicularly on the crack contour surface. The reconstruction procedure of the potential strain energy surfaces for two sections of plates y = 0 and z = 0, and the graphical presentation of these surfaces, are carried out. Based on the reconstructed potential strain energy surfaces, isoenergy lines in the region in front of the crack tip for both the analyzed examples, are obtained. It is observed that the distribution of stresses as well as that of potential strain energy are very similar in both cases, which indicates considerable influence of the geometric shape of the crack's contour surfaces. For comparison, stress state and potential strain energy state, which are obtained by using relations from literature, are shown.*

Key Words: *Crack, Stress Components, Potential Strain Energy Surfaces Reconstruction*

1. INTRODUCTION, FRAMEWORK

Experimental research which initially led to this idea was realized in 1992, 1995, 1996 and 1997 in the Laboratory for Experimental Mechanics of the University of Waterloo in Canada, under the supervision of J. T. Pindera[7], [8] and [9]. During 1997, 1998, 1999,

Received November 30, 2013
Corresponding author: Dragan B. Jovanović
Faculty of Mechanical Engineering, A. Medvedeva 14, 18000 Niš, Serbia
E-mail: jdragan@masfak.ni.ac.rs
Acknowledgements: This work was supported by the Ministry of Education and Science, Republic of Serbia, through the project ON174011, and the Faculty of Mechanical Engineering, University of Niš.

due to the impossibility of conducting conduct an experiment under real physical conditions, I decided to carry out a numerical experiment using the finite elements method and ALGOR software package that was at that time available at the Faculty of Mechanical Engineering in Niš. On the basis of the results of numerical experiments providing for an assessment of the stress and strain state in the vicinity of the crack in the plate, the aim was to confirm or refute some of the assumptions that I made during the experimental research in Canada. The first results of this research on the basis of numerical experiments have been published in the papers [4], [5], and before that in [3]. During the review of the work [5], which was published in 2002, I learned about the work of Parsons, Hall, and Rosakis [6] from the University of Pasadena (California Institute of Technology), dealing with a three-dimensional stress state and the state of deformation around the crack tip, where the finite element method was applied. This paper did not analyze or reconstruct energy distribution of deformation around the crack tip, but only stress and strain state. The authors used a multigrid method in paper [6], but it was not the same as the method that I used. All of that indicated that there were thoughts that went in a similar direction. At the same time, I learned about the work of G. C. SIH and Lee, which dealt with a three-dimensional stress state and condition of volumetric energy density (volume energy density) in the vicinity of the crack.

2. RECONSTRUCTION PROCEDURE OF THE STRAIN ENERGY SURFACE

The reconstruction procedure of the potential energy surface had previous steps, the first of which was the modeling of a crack in the plate. That means a choice between different forms of an initial crack (Figs. 1, 2), definition of boundary conditions on the crack contour, the use of symmetry that exists in geometry, and load distribution, and the choice of finite elements that will be used in the analysis of the problem.

The second step in the work was the calculation of the distribution of stress components in the plate, for the assumed global stress state and the assumed shape of the crack. Software packages were used for this. Data obtained in this way were used to graphically display the obtained stress distribution (Figs. 3, 4, 5, 6, 7, 8) as the basis for determining the value of stress components and component displacements in selected directions and in selected sections. The third step in the work was editing of data in units that were needed for further work. The fourth step was a graphical representation of curves that describe the distribution of stress components σ_x, σ_y, σ_z, τ_{xy}, τ_{yz}, τ_{zx} on selected directions. The fifth step was the calculation of the potential strain energy, where Equation (1) was used, and which was built into the Program DEFEN.

$$A'_{def} = \frac{1}{2E}[(\sigma_x^2 + \sigma_y^2 + \sigma_z^2) - 2\nu(\sigma_x\sigma_y + \sigma_x\sigma_z + \sigma_y\sigma_z) + 2(1+\nu)(\tau_{xy}^2 + \tau_{xz}^2 + \tau_{yz}^2)] \quad (1)$$

The sixth step was to edit the data of the potential strain energy and graphical representation of its distribution for selected directions and intersections. The seventh step was the reconstruction of the potential strain energy surface by the process of networking (gridding) of points obtained in the previous procedure. The polynomial regression procedure was also used. The procedure was repeated iteratively to obtain the spatial surface, in which the influence of the selected parameters for networking was eliminated

or imperceptible. Figs. 11 and 12 show a step in the process of reconstruction, where the density of points with predetermined values of the potential strain energy affects the result of the reconstruction. Periodic changes in the strain energy, which you can see in these Figs., starting at a distance the size of a double thickness of middle plate, or 1.5 thickness of the crack tip, are consequences of the insufficient density of points, which determined the value of the potential deformation energy, interacting with the reconstruction method. Consequently, an increase in the number of data points resulted in the ironing of surface in this part. The appearance of the surface waves or curves in the reconstruction as a result of uneven density of data points, was observed previously [7], [8], [9]. The experience from experimental research has been used to successfully overcome and resolve the problem of uneven density of the measurement points.

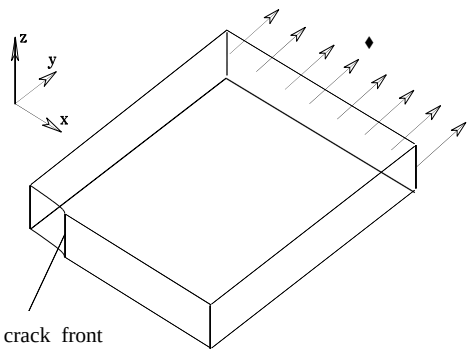

Fig. 1 Elliptical crack in the plate, loaded by normal stress σ to tension in the direction perpendicular to the crack plane, which is processed in the file PR-Z-16

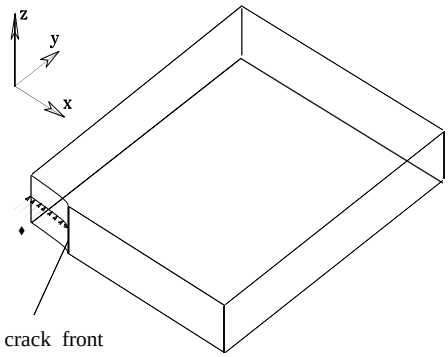

Fig. 2 Elliptical crack in the plate loaded by normal stress σ to pressure in the direction perpendicular to the crack plane, processed in the file PR-P-22

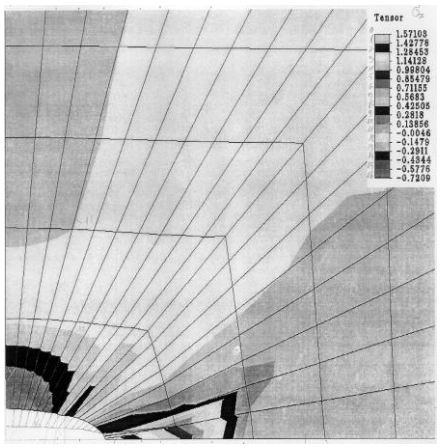

Fig. 3 PR16 normal stress distribution σ_x, for a flat cross-section z = 0, detail

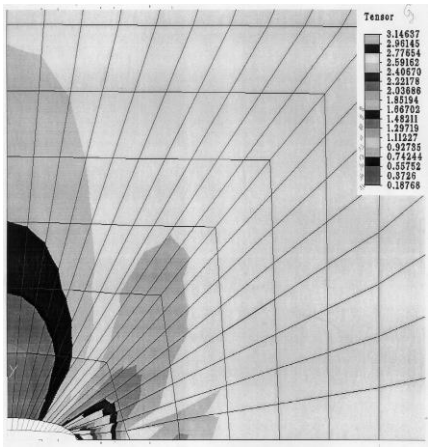

Fig. 4 PR16 normal stress distribution σ_y, for a flat cross-section z = 0, detail.

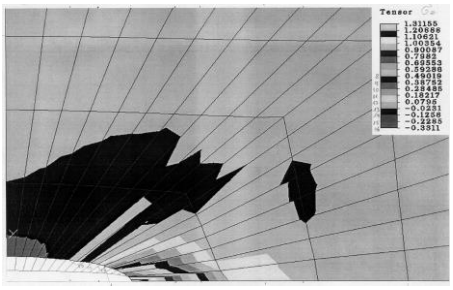

Fig. 5 PR16 normal stress distribution σ_z, for a flat cross-section z = 0, detail

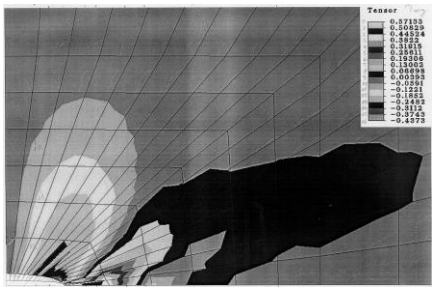

Fig. 6 PR16 shear stress distribution τ_{xy}, for a flat cross-section z = 0, detail

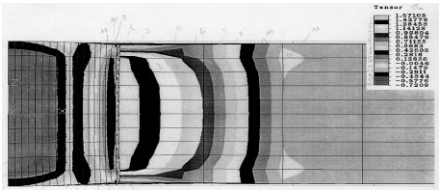

Fig. 7 PR16 normal stress distribution σ_x, for a flat cross-section **y = 0**, detail

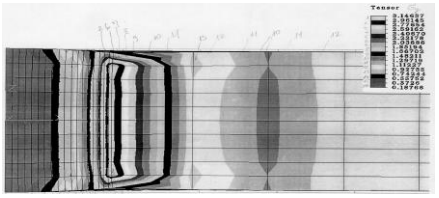

Fig. 8 PR16 normal stress distribution σ_y, for a flat cross-section **y = 0**, detail

Figs. 9 and 10 show the distribution of the potential strain energy for selected directions z = 0 mm, z = 1 mm of the intersection y = 0 mm. Then, data files are merged into a single file with data on potential strain energy of the flat section defined by y = 0 mm. Then, I made a series of iterative steps, which reconstructed the surface describing the potential energy distribution in the plane y = 0 mm, as shown in Figs. 11 and 12.

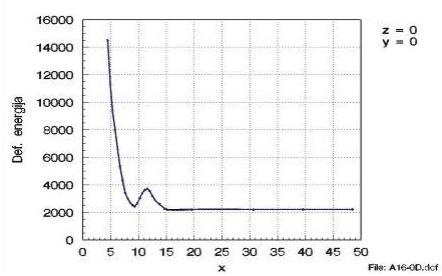

Fig. 9 Diagram of the specific strain energy in the direction determined by coordinates z = 0 mm and y = 0 mm

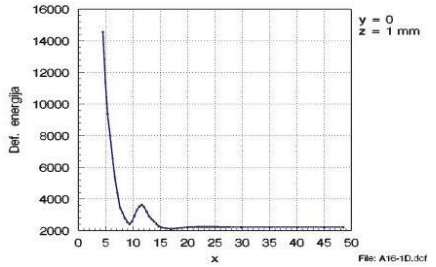

Fig. 10 Diagram of the specific strain energy in the direction determined by coordinates z = 1 mm and y = 0 mm

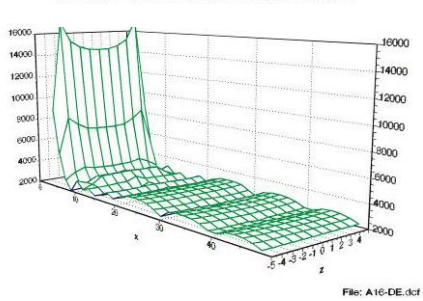

Fig. 11 Diagram of the surface of the specific strain energy of the flat section for coordinate y = 0 mm, in front of the crack's front line (the previous step of reconstruction)

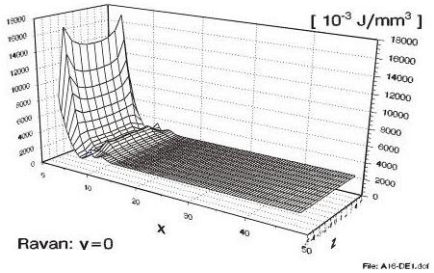

Fig. 12 Diagram of the surface of the specific strain energy of the flat section for coordinate y = 0 mm, in front of the crack's front line (the final form of reconstruction)

Fig. 13 shows a diagram of the potential strain energy in direction x = 4.5 mm, and plane cross-section y = 0 mm. This diagram shows that minimum of potential strain energy ahead of the crack in the middle of the plate cross-section, and maximums near the outer plate surfaces. This fact suggests that the points on the crack's front line, which are located near the outer plate surface will have crack propagation before the middle of the cross section of the plate.

Fig. 14 shows the iso energy lines in the cross section at z coordinates. These lines show the constant value of the potential energy of deformation, illustrating the distribution and concentration of potential strain energy, and hence point to the places where crack propagation can be expected. Fig. 15 shows a step in the iterative procedure.

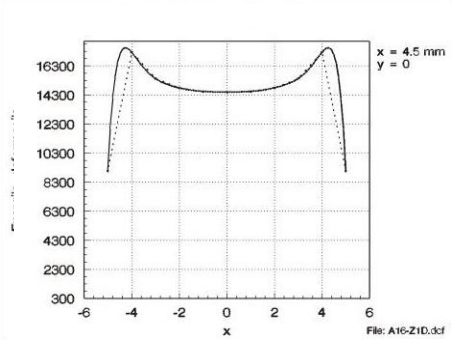

Fig. 13 Diagram of the specific strain energy in direction determined by the coordinates x = 4.5 mm and y = 0 mm

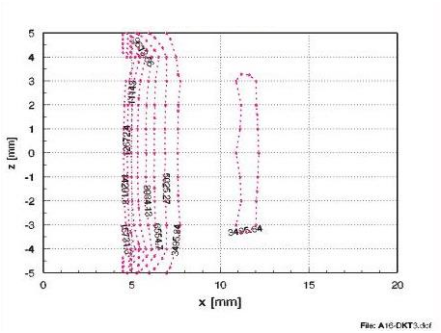

Fig. 14 Diagram of the isoenergy lines in front of crack in plane section of plate, coordinate y = 0 mm

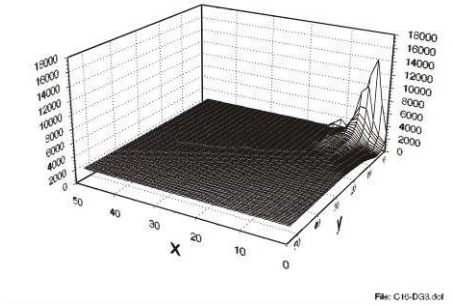

Fig. 15 Diagram of the specific strain energy for flat section of plate, coordinate z = 0 mm (the previous step reconstruction)

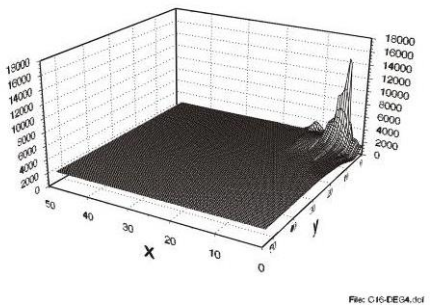

Fig. 16 Diagram of the specific strain energy for flat section of plate, coordinate z = 0 mm (the final step of reconstruction)

Fig. 16, which represents the distribution of the potential strain energy in the middle plane, shows peak energy A'_{def} = 14517·10^{-3} J/mm^3 in front of the front line of crack, which is, like in the diagram in Fig. 12. Also noted is the existence of local extreme strain energy at a distance 12 mm from the origin. This local peak energy is a consequence of the change in the law of normal stress, which at that point has a local extreme. At this point the value of the potential strain energy is much smaller than the value at the crack tip.

Figs. 17 and 18 show the isoenergy lines for middle plane of plates, where you can see the concentration of strain energy ahead of the crack tip and depression of energy field above the crack in the case PR16.

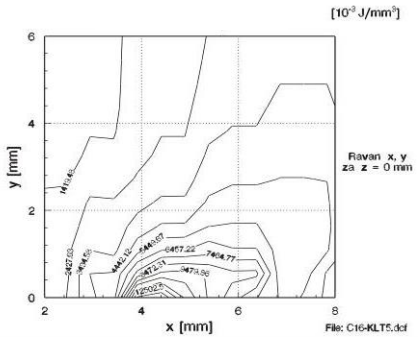

Fig. 17 PR16 Isoenergy lines in the vicinity of the crack tip, plane of section (x–y) for z = 0 mm (shown in enlarged detail)

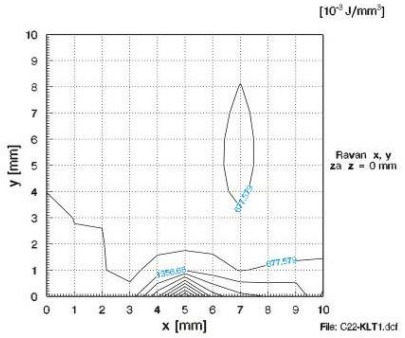

Fig. 18 PR22 Isoenergy lines in the vicinity of the crack tip, plane of section (x–y) for z = 0 mm (shown in enlarged detail)

3. Stresses and Strain Energy in front of the Crack Tip According to the Literature

Compare the results with graphical display of stress and deformation potential energy obtained from the relation to the Refs. [1] and [2]. D. Broek on page 95 Ref. [1] Elementary Engineering Fracture Mechanics gives relations for stresses, in the polar system of coordinates:

$$\sigma_x = \frac{K_I}{\sqrt{2\pi r}} \cos\frac{\theta}{2}\left(1 - \sin\left(\frac{\theta}{2}\right)\cdot\sin\left(\frac{3\theta}{2}\right)\right) \tag{2}$$

$$\sigma_y = \frac{K_I}{\sqrt{2\pi r}} \cos\frac{\theta}{2}\left(1 + \sin\left(\frac{\theta}{2}\right)\cdot\sin\left(\frac{3\theta}{2}\right)\right) \tag{3}$$

$$\tau_{xy} = \frac{K_I}{\sqrt{2\pi r}} \cos\frac{\theta}{2}\sin\frac{\theta}{2}\cdot\sin\frac{3\theta}{2} \tag{4}$$

$\sigma_z = 0$, for the plane stress state and

$$\sigma_x = \nu(\sigma_x + \sigma_y)\text{, in the case of plane deformation} \tag{5}$$

Broek says that in many cases is $K_I = \sigma\sqrt{\pi a}$, regardless of the size effect of the object, where: σ – tensile stress of the external load, a – greater semi-axis length of ellipse as shown in Fig. 19.

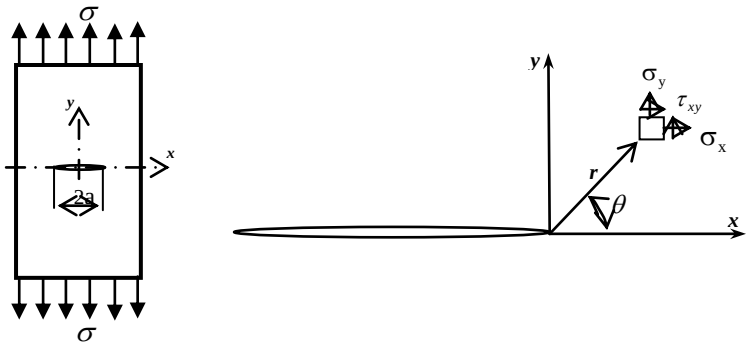

Fig. 19 Axially loaded plate with crack length 2*a* and coordinate system (x, y) and (*r*, *θ*) (in front of the crack tip from Ref. [1]).

Firstly, it should be indicated in these solutions that they start from an assumed plane stress or strain in the plate at the crack tip vicinity. All these solutions are based on the assumption that the stress state in front of the crack is critical for crack propagation, not the potential strain energy status or the energy density distribution state in the vicinity of the crack.

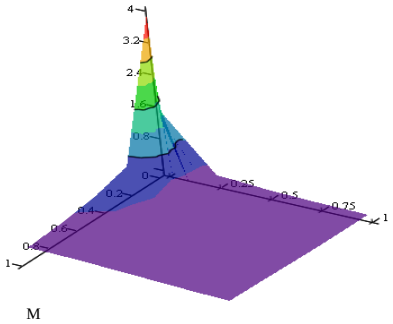

Fig. 20 Distribution of normal stress σ_x, in coordinate system (x, y)

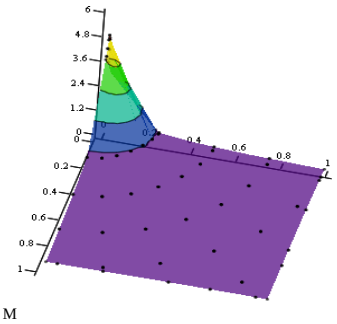

Fig. 21 Distribution of normal stress σ_y, in coordinate system (x, y)

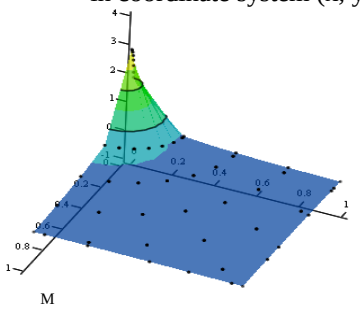

Fig. 22 Distribution of normal stress σ_z, in coordinate system (x, y)

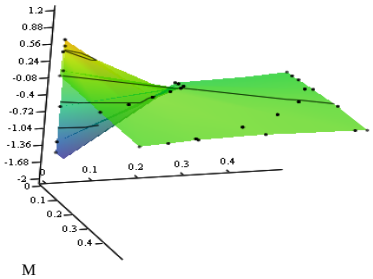

Fig. 23 Distribution of shear stress τ_{xy}, in coordinate system (x, y)

Based on the stress values obtained from equations (2), (3), (4) and (5) and by using the expression for the potential strain energy (1) from the literature a diagram of the potential strain energy is obtained, shown in Fig. 24.

Pronounced linearity of this graph does not correspond to the real physical conditions, because the potential strain energy distribution around the crack tip as well as distribution of stresses is non-linear. Nonlinearity of stresses has been demonstrated in experimental [7], [8], [9] and analytical studies.

Stress concentration should no longer be seen as a criterion for determining the crack propagation direction and site, but the potential strain energy concentration.

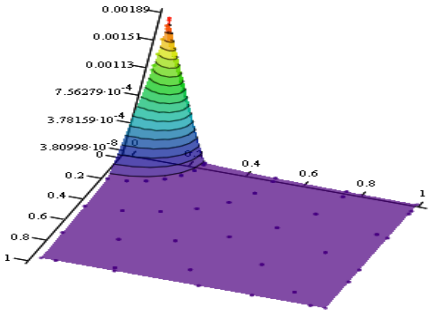

Fig. 24 Distribution of potential strain energy A_{def} ahead of the crack tip in coordinate system (x, y).

We can compare the results of reconstruction with the graphical presentation of potential strain energy obtained from the relations (6), from Refs. [1], [2]. Gdoutos on page 34 of Ref. [2] Fracture Mechanics - An Introduction, gives relations for stresses, in the polar system of coordinates of the form of crack propagation type I (opening):

$$\sigma_x(r,\varphi)=\left(\frac{K_I}{\sqrt{2\cdot\pi\cdot r}}\right)\cdot\left(\cos\left(\frac{\varphi}{2}\right)\right)\cdot\left[1-\left(\sin\left(\frac{\varphi}{2}\right)\right)\cdot\left(\sin\left(\frac{3\varphi}{2}\right)\right)\right]$$

$$\sigma_y(r,\varphi)=\left(\frac{K_I}{\sqrt{2\cdot\pi\cdot r}}\right)\cdot\left(\cos\left(\frac{\varphi}{2}\right)\right)\cdot\left[1+\left(\sin\left(\frac{\varphi}{2}\right)\right)\cdot\left(\sin\left(\frac{3\varphi}{2}\right)\right)\right]$$

$$\sigma_z(r,\varphi)=0$$

$$\tau_{xy}(r,\varphi)=\left(\frac{K_I}{\sqrt{2\cdot\pi\cdot r}}\right)\cdot\left(\sin\left(\frac{\varphi}{2}\right)\right)\cdot\left[\left(\cos\left(\frac{\varphi}{2}\right)\right)\cdot\left(\cos\left(\frac{3\varphi}{2}\right)\right)\right]$$

$$\tau_{xz}(r,\varphi)=0,\quad \tau_{yz}(r,\varphi)=0\quad . \tag{6}$$

By applying previous relations (6) we get the distribution of potential strain energy ahead of the crack tip shown in Fig. 25. (a, b, c).

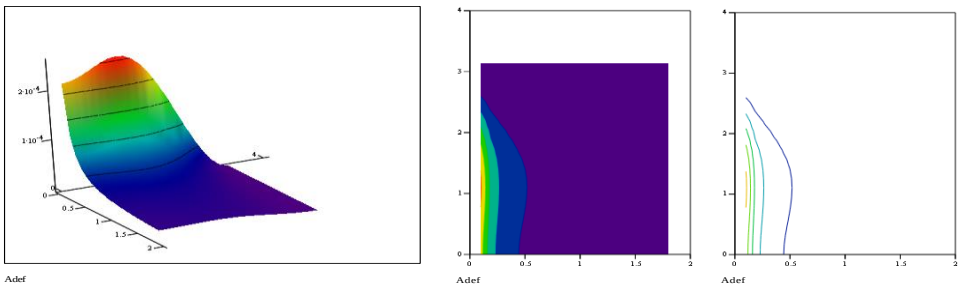

Fig. 25 a) Surface of potential strain energy obtained by relations (6), (type I)
b) The projection of the potential strain energy surface at *x*-*y* plane.
c) Isoenergy lines in front of the crack tip.

By superposition of type I and type II forms of crack propagation, relations are obtained for the combination of the two cases of stress states, from Refs. [1], [2]:

$$\sigma_x(r,\varphi)=\left(\frac{K_I}{\sqrt{2\cdot\pi\cdot r}}\right)\cdot\left(\cos\left(\frac{\varphi}{2}\right)\right)\cdot\left[1-\left(\sin\left(\frac{\varphi}{2}\right)\right)\cdot\left(\sin\left(\frac{3\varphi}{2}\right)\right)\right]-\left(\frac{K_{II}}{\sqrt{2\cdot\pi\cdot r}}\right)\cdot$$
$$\cdot\left(\sin\left(\frac{\varphi}{2}\right)\right)\cdot\left[2+\left(\cos\left(\frac{\varphi}{2}\right)\right)\cdot\left(\sin\left(\frac{3\varphi}{2}\right)\right)\right]$$

$$\sigma_y(r,\varphi)=\left(\frac{K_I}{\sqrt{2\cdot\pi\cdot r}}\right)\cdot\left(\cos\left(\frac{\varphi}{2}\right)\right)\cdot\left[1-\left(\sin\left(\frac{\varphi}{2}\right)\right)\cdot\left(\sin\left(\frac{3\varphi}{2}\right)\right)\right]-\left(\frac{K_{II}}{\sqrt{2\cdot\pi\cdot r}}\right)\cdot$$
$$\cdot\left(\sin\left(\frac{\varphi}{2}\right)\right)\cdot\left[\left(\cos\left(\frac{\varphi}{2}\right)\right)\cdot\left(\sin\left(\frac{3\varphi}{2}\right)\right)\right]$$

$$\sigma_z(r,\varphi)=\nu\cdot(\sigma_x(r,\varphi)+\sigma_y(r,\varphi)),\quad \tau_{xz}(r,\varphi)=0,\quad \tau_{yz}(r,\varphi)=0$$

$$\tau_{xy}(r,\varphi)=\left(\frac{K_I}{\sqrt{2\cdot\pi\cdot r}}\right)\cdot\left(\sin\left(\frac{\varphi}{2}\right)\right)\cdot\left[\left(\cos\left(\frac{\varphi}{2}\right)\right)\cdot\left(\cos\left(\frac{3\varphi}{2}\right)\right)\right]+$$
$$+\left(\frac{K_{II}}{\sqrt{2\cdot\pi\cdot r}}\right)\cdot\left(\cos\left(\frac{\varphi}{2}\right)\right)\cdot\left\{1-\left[\left(\sin\left(\frac{\varphi}{2}\right)\right)\cdot\sin\left(\frac{3\varphi}{2}\right)\right]\right\} \tag{7}$$

By applying previous relations (7) we obtain distribution of the potential strain energy ahead of the crack tip, for the combination of type I and type II form of crack propagation, shown in Fig. 26 (a, b, c).

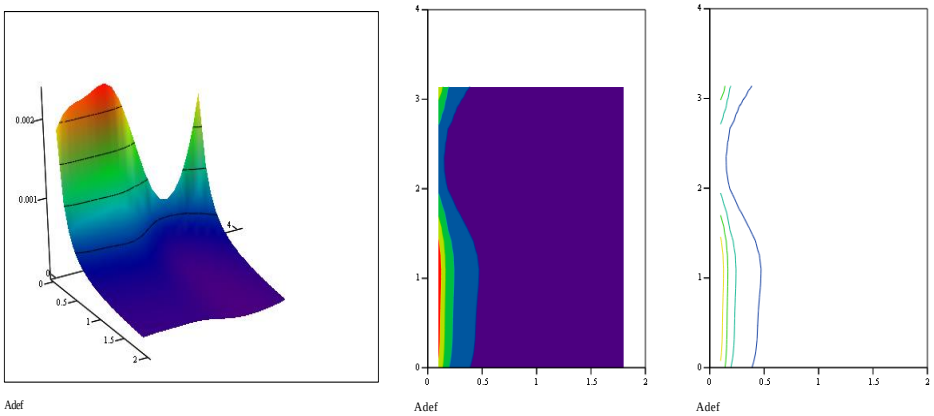

Fig. 26 a) Surface of potential strain energy by relations (7), (type I and type II)
b) The projection of the potential strain energy surface at *x*-*y* plane.
c) Isoenergy lines in front of the crack tip

4. CONCLUSIONS

The results of applying the idea of reconstructing the spatial surface, that describes the potential strain energy distribution in the crack vicinity, are presented. In particular, I have analyzed the examples of cracks identified in the paper as PR-Z-16 and PR-P-22. Geometry of the cracks and plates are completely the same. I have selected the same finite element mesh for stress calculation in both cases. The only difference between the examples is the way of loading the plate. In example of PR-Z-16 plate is loaded in the axial direction of Y axis and perpendicular to the direction of the crack plane. While, in the case of PR-P-22 the plate is loaded with a continuous load on the crack surface contour. Based on the reconstructed potential strain energy surface I got the isoenergy lines in front of the crack tip, for both analyzed examples. It is observed that the distribution of stresses, as well as that of the potential strain energy are very similar in both cases, indicating the main role of geometric shape of contour surface of the crack. Finally, I have showed the comparison of stress and potential strain energy surfaces, which are based on the relations from the literature.

REFERENCES

1. Broek D., 1982, *Elementary Engineering Fracture Mechanics*, Martinus Nijhoff Publishers, The Hague.
2. Gdoutos E. E., 1993, *Fracture Mechanics*, Kluwer Academic Publishers, Dordrecht, 369 p.
3. Jovanović D. B., Jovanović M., 2000, *Local stress and strain state in the region of crack for different global stress states in a plate*, YUSNM, Niš 2000, Facta Universitatis, Series Mechanical Engineering, Vol. 1, No. 7, pp 925-934.
4. Jovanović D. B., Jovanović M., 2001, *Stress state and strain energy distribution at the vicinity of elliptical crack with compression forces acting on it's contour*, Facta Universitatis, Series Mechanics, Automatic Cont. and Rob., Vol. 3, No.11, pp. 223-230.
5. Jovanović D. B., 2002, *Stress state and deformation (strain) energy distribution ahead crack tip in a plate subjected to tension*, Facta Universitatis., Series Mechanics, Automatic Control and Robotics, Vol. 3, No. 12, pp. 443-455.
6. Parsons I. D., Hall J. F., Rosakis A. J., 1986, *A Finite Element Investigation of the Elastostatic State Near a Three Dimensional Edge Crack*, SM Report 86-29, Division of Engineering and Applied Science, California Institute of Technology, Pasadena, California.
7. Pindera J. T., Josepson J., Jovanović D.B., 1996, *Electronic Techniques in Isodyne Stress Analysis*, Abstract Proceedings of the VIII International Congress on Experimental Mechanics, Nashville, USA.
8. Pindera J. T., Josepson J., Jovanović D.B., 1997, *Electronic Techniques in Isodyne Stress Analysis: Part 1. Basic Relations*, Experimental Mechanics, Vol. 37, No. 1, 33-38.
9. Pindera J. T., Josepson J., Jovanović D.B., 1997, *Electronic Techniques in Isodyne Stress Analysis: Part 2. Illustrating Studies and Discussion*, Experimental Mechanics, Vol. 37, No. 2, 106-110.

POVRŠINE POTENCIJALNE ENERGIJE DEFORMACIJE U OKOLINI VRHA PRSLINE

U radu su prikazani rezultati i osnovni elementi postupka rekonstrukcije površi potencijalne energije deformacije u okolini prsline. Ukazano je na izvesna ograničenja i specifičnosti metode u procenjivanju krivih i trodimenzionalnih površi koje se najbolje uklapaju sa podacima za komponente napona i potencijalnu energiju deformacije. Analiziraju se primeri prsline potpuno istih geometrija prsline i ploče, koji su u radu imenovani kao PR-Z-16 i PR-P-22. Izabrana je ista mreža konačnih elemenata za proračun u oba slučaja. Prvi primer ploče je opterećen naponom σ u y - pravcu na spoljašnjoj ivici ploče, upravno na ravan prsline, dok je u primeru PR-P-22 ploča opterećena naponom σ kontinualno i upravno na površ konture prsline. Realizovan je postupak rekonstrukcije površi potencijalne energije deformacije za dva preseka ploče y = 0 i z = 0, a urađen je i grafički prikaz ovih površi. Na osnovu rekonstruisanih površi potencijalne energije deformacija dobijene su izoenergijske linije u oblasti ispred čela prsline, za oba alalizirana primera. Uočava se sličnost rasporeda napona, kao i rasporeda potencijalne energije deformacije za oba slučaja, što ukazuje na značajan uticaj geometrijskog oblika konturne površi prsline. Prikazani su za upoređenje stanje napona i stanje potencijalne energije deformacije koji su dobijeni korišćenjem relacija iz literature.

Ključne reči: *prslina, komponentni naponi, rekonstrukcija površi potencijalne energije deformacije*